AFRL-ML-WP-TP-2007-463

E-BEAM-CURED LAYERED-SILICATE AND SPHERICAL SILICA EPOXY NANOCOMPOSITES (PREPRINT)

Chenggang Chen
David P. Anderson

MARCH 2007

Approved for public release; distribution unlimited.

STINFO COPY

This work was funded in whole or in part by Department of the Air Force contract FA8650-05-D-5052. The U.S. Government has for itself and others acting on its behalf an unlimited, paid-up, nonexclusive, irrevocable worldwide license to use, modify, reproduce, release, perform, display, or disclose the work by or on behalf of the U.S. Government.

MATERIALS AND MANUFACTURING DIRECTORATE
AIR FORCE RESEARCH LABORATORY
AIR FORCE MATERIEL COMMAND
WRIGHT-PATTERSON AIR FORCE BASE, OH 45433-7750

NOTICE AND SIGNATURE PAGE

AFRL-ML-WP-TP-2007-463 HAS BEEN REVIEWED AND IS APPROVED FOR PUBLICATION IN ACCORDANCE WITH ASSIGNED DISTRIBUTION STATEMENT.

*//Signature//

AJIT K. ROY, Project Engineer
Structural Materials Branch
Nonmetallic Materials Division

//Signature//

KEITH B. BOWMAN, Acting Chief
Structural Materials Branch
Nonmetallic Materials Division

//Signature//

SHASHI K. SHARMA, Acting Deputy Chief
Nonmetallic Materials Division
Materials and Manufacturing Directorate

This report is published in the interest of scientific and technical information exchange, and its publication does not constitute the Government's approval or disapproval of its ideas or findings.

*Disseminated copies will show "//Signature//" stamped or typed above the signature blocks.

REPORT DOCUMENTATION PAGE

Form Approved
OMB No. 0704-0188

1. REPORT DATE *(DD-MM-YY)*	2. REPORT TYPE	3. DATES COVERED *(From - To)*
March 2007	Journal Article Preprint	

4. TITLE AND SUBTITLE
E-BEAM-CURED LAYERED-SILICATE AND SPHERICAL SILICA EPOXY NANOCOMPOSITES (PREPRINT)

5a. CONTRACT NUMBER
FA8650-05-D-5052

5b. GRANT NUMBER

5c. PROGRAM ELEMENT NUMBER
62102F

6. AUTHOR(S)
Chenggang Chen
David P. Anderson

5d. PROJECT NUMBER
4347

5e. TASK NUMBER
RG

5f. WORK UNIT NUMBER
M03R1000

7. PERFORMING ORGANIZATION NAME(S) AND ADDRESS(ES)
University of Dayton Research Institute
300 College Park
Dayton OH 45469

8. PERFORMING ORGANIZATION REPORT NUMBER

9. SPONSORING/MONITORING AGENCY NAME(S) AND ADDRESS(ES)
Materials and Manufacturing Directorate
Air Force Research Laboratory
Air Force Materiel Command
Wright-Patterson AFB, OH 45433-7750

10. SPONSORING/MONITORING AGENCY ACRONYM(S)
AFRL-ML-WP

11. SPONSORING/MONITORING AGENCY REPORT NUMBER(S)
AFRL-ML-WP-TP-2007-463

12. DISTRIBUTION/AVAILABILITY STATEMENT
Approved for public release; distribution unlimited.

13. SUPPLEMENTARY NOTES
Journal article submitted to the Journal of Applied Polymer Science. This work was funded in whole or in part by Department of the Air Force contract FA8650-05-D-5052. The U.S. Government has for itself and others acting on its behalf an unlimited, paid-up, nonexclusive, irrevocable worldwide license to use, modify, reproduce, release, perform, display, or disclose the work by or on behalf of the U.S. Government.

PAO Case Number: AFRL/WS 07-0503, 02 Mar 2007. Paper contains color content.

14. ABSTRACT
This research demonstrates than an epoxy nanocomposite can be made through electron beam (e-beam) curing. The nanofillers can be two dimensional (layered-silicate) and zero dimensional (spherical silica). Both the spherical silica epoxy nanocomposite and the layered-silicate epoxy nanocomposite can be cured to a high degree of curing. The transmission electron microscopy (TEM) and small-angle x-ray scattering (SASX) of the e-beam-cured layered-silicate epoxy nanocomposites demonstrate the intercalated nanostructure or combination of exfoliated and intercalated nanostructure. The TEM images show that the spherical silica epoxy nanocomposite has the morphology of homogeneous dispersion of aggregates of silica nanoparticles. The aggregate size is ~100nm. The dynamic mechanical analysis shows that the storage modulus of the spherical silica nanocomposite has been improved, and the glass transition temperature can be very high (~175 °C).

15. SUBJECT TERMS
Nanocomposite, electron beam curing, epoxy, morphology

16. SECURITY CLASSIFICATION OF:			17. LIMITATION OF ABSTRACT:	18. NUMBER OF PAGES	19a. NAME OF RESPONSIBLE PERSON (Monitor)
a. REPORT	b. ABSTRACT	c. THIS PAGE			Ajit K. Roy
Unclassified	Unclassified	Unclassified	SAR	30	19b. TELEPHONE NUMBER *(Include Area Code)* N/A

Standard Form 298 (Rev. 8-98)
Prescribed by ANSI Std. Z39-18

E-Beam-Cured Layered-Silicate and Spherical Silica Epoxy Nanocomposites

Chenggang Chen and David P. Anderson*

University of Dayton Research Institute, 300 College Dayton, OH 45469-0168

E-mail: Chenggang.Chen@wpafb.af.mil

ABSTRACT

This research demonstrates that an epoxy nanocomposite can be made through electron beam (e-beam) curing. The nanofillers can be two dimensional (layered-silicate) and zero dimensional (spherical silica). Both the spherical silica epoxy nanocomposite and the layered-silicate epoxy nanocomposite can be cured to a high degree of curing. The transmission electron microscopy (TEM) and small-angle x-ray scattering (SAXS) of the e-beam-cured layered-silicate epoxy nanocomposites demonstrate the intercalated nanostructure or combination of exfoliated and intercalated nanostructure. The TEM images show that the spherical silica epoxy nanocomposite has the morphology of homogeneous dispersion of aggregates of silica nanoparticles. The aggregate size is ~100 nm. The dynamic mechanical analysis shows that the storage modulus of the spherical silica nanocomposite has been improved, and the glass transition temperature can be very high (~175°C).

KEYWORDS: nanocomposite; electron beam curing; epoxy; morphology

1. INTRODUCTION

The research on polymeric materials reinforced by nanofillers has exploded in the last two decades [1-6]. Nanofillers generally have an extremely large surface-to-volume ratio, and the coupling from the extremely large interfacial areas between the polymer and nanofiller could assist stress transfer to the nanophase filler to make high-performance nanocomposite materials [4]. Simultaneously, the synergistic effects from the soft polymeric phase and hard inorganic phase make this type of material exhibit unique morphology and properties. The polymeric materials reinforced by nanofillers can provide the properties that traditional composites cannot. The factors affecting the properties of the polymeric nanocomposite materials include the type, particle shape and size, morphology, and concentration of the fillers. The nanofiller materials widely used today are nanosized carbon particles, spherical nanosilica and polyhedral oligomeric silsequioxane (POSS) (zero-dimensional); carbon nanotube, carbon nanofiber and silica nanotube (one-dimensional); and silicate nanolayers and graphite (two-dimensional) [1-6]. In this paper, the nanofiller used is spherical nanosilica or nanoclay.

Epoxy resin is a very common and widely used thermosetting material. Recently, the research on inorganic particulate-filled epoxy composites has been very active in improving the mechanical, barrier, electrical, magnetic, thermal, thermoxidation, flame retardancy, and optical properties [2-22]. In almost all the reported epoxy nanocomposites, it contains an epoxy resin, curing agent, and nanofillers, and was made through a traditional thermal curing procedure [2-22]. However, radiation curing of the epoxy resin and traditional carbon fiber composites by e-beam has recently attracted great interest [23-34]. The e-beam curing technology provides many advantages over the traditional thermal curing processing. An e-beam accelerator produces ionic species, free radicals and molecules in excited states. The advantages of the e-beam curing

technology include shorter curing time, lower shrinkage, lower tooling cost, improved performance, greater production flexibility, reduction of volatile organic compounds, elimination of the typical hazardous and sometimes carcinogenic curing agents and is therefore more environmentally friendly [23-33]. It is of great interest and significance to cure the spherical silica epoxy nanocomposites and layered-silicate epoxy nanocomposites through e-beam cure technology. However, up to now, there have been very few reports for the e-beam-cured layered-silicate epoxy nanocomposite and spherical silica epoxy nanocomposite. This is probably due to the small overlap of experts in the two different fields of nanocomposite material and e-beam curing technology. In addition, the organoclay, especially the commercial organoclay, used for making layered-silicate epoxy generally contains small amounts of nucleophilic amine. The amines are known to poison the cationic catalysts used in e-beam cure. Our earlier research reported an initial example of e-beam-cured intercalated layered-silicate epoxy nanocomposite [34]. Here the preparation of the layered-silicate epoxy nanocomposites and spherical silica epoxy nanocomposite through e-beam curing will be reported. The degree of curing after e-beam curing was checked with differential scanning calorimetry (DSC) studies, and the nanostructure of the e-beam-cured epoxy nanocomposite was verified through TEM and SAXS studies.

2. EXPERIMENTAL

2.1 MATERIALS

Epon 862 (a bis-phenol F epoxy), Epon 828 (a bis-phenol A epoxy), and curing agent W (diethyltoluenediamine) were purchased from Miller-Stephenson Chemical Company, Inc. The nanosized spherical silica is fumed silica powder (14 nm), which was obtained from the Aldrich

Company. SNA and S30B were obtained from Southern Clay Products. I.30E was obtained from Nanocor. SC8 was prepared through ion-exchange chemistry by the treatment of SNA (CEC: ~ 92 meq/100g) with *n*-octylamine and HCl in the water-ethanol mixed solvent. E-beam catalyst ([4-[(2-hydroxytetradecyl)oxy]phenyl] phenyliodium hexafluoroantimonate), CD1012, was obtained from Applied Poleramic, Inc.

2.2 PREPARATION OF NANOCOMPOSITE SAMPLE

The nanoparticles with Epon 862 or Epon 828 were mixed thoroughly using a high-shear mixing procedure (IKA ULTRA-TURRAX T25 mixer, 13500 rpm) in the presence of acetone in a bath sonicator over two hours. After the acetone was mostly evaporated, the resulting mixture was ultrasonicated (ultrasonication probe, Fisher Scientific, 60 Sonic Desmembrator, frequency: 22.5 KHz, the out power is 12 W) for an additional hour. The acetone in the mixture was then completely evaporated. The e-beam catalyst (CD1012, 1 wt.% loading) was added, and the mixture was mixed with a magnetic stir-bar. The resultant mixture was then combined with a molecular sieve to ensure that the mixture was dried. All procedures after addition of the e-beam catalyst were performed in a dark or dim environment.

The e-beam curing was performed at the National Composites Center, Kettering, Ohio. Samples were exposed to the electron beam in an EB-10™ Series High Energy Electron Beam Processing System manufactured by Electron Solutions Inc. The e-beam was set to deliver pulses or constant beam at a calibrated ~6 kGy/min. The samples were poured into silicone on a flat plate. Ethylene glycol fluid at a constant temperature (30°C) was circulated throughout the plate. The plate and samples were moved back and forth through the e-beam so as to apply a total of 150 kGy dosage to the samples over 45 minutes. The constant temperature fluid and

sample moving was used to control the exothermic epoxy reaction to prevent the temperature in the samples from rising above 80°C.

2.3 CHARACTERIZATION

Wide-angle x-ray diffraction (WAXD) was performed in the Rigaku x-ray powder diffractometer. The generator power (Cu Kα radiation) was 40 kV and 150 mA, the scan was from 2° to 10°, and the scan mode was continuous with a scan rate of 0.8°/min. SAXS was performed in a Bruker AXS with a GADDS Hi-Sta 2D detector. The radiation was Cu Kα and the power was 40 kV and 40 mA. The sample for TEM was microtomed in a Reichert-Jung Ultracut Microtome and mounted on 200-mesh copper grids. TEM was performed using a Philips CM200 transmission electron microscope. The dynamic mechanical analysis was performed using a RHEOMETRICS ARES dynamic spectrometer using torsion bar geometry at a frequency of 100 rad/sec, a strain of 1%, and a heating rate of 2°C/min. DSC was performed on a TA Instruments differential scanning calorimeter 2920 modulated DSC at 2°C/min with nitrogen sweep gas.

3. RESULTS AND DISCUSSION

3.1 E-BEAM CURING:

The electron beam excites the catalyst which then reacts with an epoxy monomer; the growing end then becomes the excited site. This active site opens up the next epoxide ring and extends the chain until termination. The degrees of cure (α) or fraction of epoxide rings opened in the e-beam samples were calculated based on the exothermic heat liberated during the DSC run (completing the cure thermally).

$$\alpha = 1 - \Delta H_{after} / \Delta H_{control}$$

ΔH_{after} is the exothermic heat of the sample after e-beam curing, while $\Delta H_{control}$ is the exothermic heat of the sample without e-beam cure.

All the data of the calculated curing degree of the e-beam-cured samples are shown in Table 1. The degrees of cure of the pure Epon 862 or Epon 828 with catalyst CD1012 (1 wt.%) were 86% and 77%, those of the nanocomposite with spherical silica nanoparticle were 79% and 73%; and that of the nanocomposite with layered-silicate was from 63% to 69%. The slight decrease of the degree of cure of the spherical silica epoxy nanocomposite is likely due to the existence of silanol groups in the silica nanoparticles. The further decrease of the degree of cure in the layered-silicate nanocomposites is probably due to the very small amount of amine existing in the organoclay in addition to the silanol group in organoclay. However, overall the degree of cure of all these samples was very good.

3.2 NANOSTRUCTURE OF THE EPOXY NANOCOMPOSITE

The TEM images were obtained on the spherical silica epoxy nanocomposite cured by e-beam. The TEM images of 1.5 wt.% SiO_2/Epon 862/CD1012 at several magnifications are shown in Figure 1. The images, especially at low magnification, show that the spherical silica particle clusters are homogeneously dispersed in the epoxy matrix. The silica nanoparticles appear as dark dots. The size of the homogeneous dispersion is in the size range of ~100 nm, and the spherical silica nanoparticles are still in an aggregated state. Each aggregation contains several to about 10 individual particles. The individual silica nanoparticles are around 15 nm, which is very close to the 14-nm size of the silica nanoparticle reported by the manufacturer. So the morphology of the e-beam-cured nanocomposite is a homogeneous dispersion of the

aggregated nanoparticles, which is the same as the morphology observed for the thermally-cured nanocomposite [35].

The homogeneous dispersion of the aggregated spherical silica nanoparticles is attributed to the high shear and ultasonication procedures. A general mixing procedure, such as with a magnetic stir-bar, will result in a significantly less dispersed system. In fact, for the stir-bar mixing procedure, the silica particles from Aldrich were observed partially precipitated from the mixture after standing overnight. For the high-shear mixing procedure, the mixture of the spherical silica particle and Epon 862 could be stable for several days. For the proceeding procedure of high-shear and ultrasonication, the Epon 862 mixture with the spherical nanoparticles was very stable, and no spherical silica was precipitated even after months. The mixture after the processing procedures of high shear and ultrasonication looked much clearer than those with the high-shear mixing procedure or stir-bar mixing alone. The stability of the mixture depends on the size of the dispersed silica particles. The small particle's Brownian motion inside the Epon matrix can prevent or slow the effect of gravity on the small particle. Generally, the smaller the size of the particle, the more stable the mixture will be. The higher intensity of the processing can result in more homogenous dispersion and smaller particles. This also indicates that the morphology of the nanocomposite is determined before the cure, and there is no morphology development during the curing step, which is totally different for the thermally-cured layered-silicate epoxy naocomposites [8-12].

Another example of the TEM images of the cured spherical silica epoxy nanocomposite (1.3 wt.% SiO_2/Epon 862/CD1012) is shown in Figure 2. The morphology of this spherical silica epoxy nanocomposite is very similar to that of 1.5 wt.% SiO_2/Epon 862/CD1012

nanocomposite. The morphology of the nanocomposite is that of a homogeneous dispersion of the aggregated nanoparticles.

The TEM images of the e-beam-cured 4.0 wt.% SC8/Epon 862/CD1012 layered-silicate epoxy nanocomposite at low magnification and high magnification are shown in Figure 3. The layered-silicate is well dispersed in the epoxy matrix. Most of the silicate nanolayers are individual or 2 to 5 nanolayers, while some of them are still in stacked aggregation, composed of more than 10 aggregations. The morphology appears as the combination of exfoliated and intercalated nanostructure. The dispersion of this nanocomposite is much better than that of our previously e-beam-cured nanocomposite 4.0 wt.% SC8/Epon 862/CD1012 [35]. The difference is caused by the different processing procedures for mixing the organoclay with Epon 862. In this research, the mixing of SC8 with Epon 862 is through the high-shear mixing in the presence of acetone and ultrasonication, while the mixing in our previous paper was by stir-bar mixing only [35]. The high-shear mixing and additional ultrasonication is very powerful and can help to break some of the aggregates into the silicate nanolayers in this 4.0 wt.% SC8/Epon 862 mixture.

The TEM images of the e-beam-cured 3.7 wt.% I.30E/Epon 862/CD1012 nanocomposite are shown in Figure 4. The silicate nanolayers are still in an aggregated state, a typical intercalated structure, although high-shear mixing and ultrasonication are applied for the processing. This is perhaps due to the more organic pendent groups inside the gallery hindering the penetration of the epoxy and acetone inside the gallery during the processing [d: 22.8 Å (I.30E) versus 13.2 Å (SC8)] and thus makes the separation and breaking of the aggregate of I.30E difficult. More research is needed to fully understand the phenomena.

For the e-beam-cured layered-silicate epoxy nanocomposite, another very common and useful characterization of the morphology is SAXS. The SAXS of these e-beam-cured layered-

silicate epoxy nanocomposites are shown in Figure 5. The (001) peak is clear in the SAXS spectra of all of these nanocomposites. All of these nanocomposites have intercalated nanostructures. The interplanar spacings between the gallery are 41 Å, 31 Å and 34 Å for the 3.7 wt.% I.30E/Epon 862/CD1012 nanocomposite, 4.0 wt.% SC8/Epon 862/CD1012 nanocomposite, and 1.0 wt.% S30B/Epon 862/CD1012 nanocomposite, respectively.

It is interesting to note the intensity of the (001) peak for these nanocomposites when the experimental conditions for the SAXS are the same. The intensity sequence for the (001) peak in SAXS decreases according to the sequence of 3.7 wt.% I.30E/Epon 862/CD1012 nanocomposite to 1.0 wt.% S30B/Epon 862/CD1012 nanocomposite, and to 4.0 wt.% SC8/Epon 862/CD1012 nanocomposite. The reason the intensity of the 3.7 wt.% I.30E/Epon 862/CD1012 nanocomposite is stronger than that of the 1.0 wt.% S30B/Epon 862/CD1012 nanocomposite seems reasonable and expected due to the higher loading of the clay in the 3.7 wt.% I.30E/Epon 862/CD1012 nanocomposite. The lowest intensity of the 4.0 wt.% SC8/Epon 862/CD1012 nanocomposite is due to the morphology of the combination of the exfoliation and intercalation, in which the exfoliated morphology is dominating as TEM shows. So although the loading for the SC8/Epon 862/CD1012 is highest (4.0 wt.%), the effective concentration of the aggregate with the intercalated nanostructure is lowest and thus has the lowest intensity of (001) peak.

Based on the characterization from TEM and SAXS of the e-beam-cured layered-silicate epoxy nanocomposite, the morphology is intercalated or a combination of exfoliation and intercalation. The partial exfoliation is caused by the very intense processing before the e-beam curing. No matter what morphology (the intercalation or combination of intercalation and exfoliation) is and what type of layered silicate is used, the interplanar spacing between the layers is smaller (~30 Å). However, the interplanar spacing of the most thermally-cured layered-

silicate epoxy nanocomposite ended with very large interplanar spacing (100 to 200 Å) [7-13, 16].

The morphology development for the layered-silicate epoxy nanocomposite through the e-beam curing is different from that of the traditional thermal curing. In the thermal curing procedure, the temperature is gradually increased, and the catalytic effect from the organic group inside the gallery makes the intragallery polymerization occur at a lower temperature [8-12]. The consumption of the intragallery epoxy monomer breaks the original equilibrium of epoxy monomer between the intragallery and extragallery and is the driving force for the migration of the epoxy resin from the extragallery into the intragallery. So the layered-silicate epoxy nanocomposite with organoclay containing the catalytic organic groups such as free ammonium cation can result in very large interplanar spacing (~100 to 200 Å), while those without a catalytic organic group such as ternary ammonium generally result in smaller interplanar spacing (~30 to 40 Å) [12]. In the e-beam curing, the epoxy resins outside the gallery of the layered silicate and inside the gallery are cured simultaneously and the curing is fast. So there will be no epoxy migration from extragallery to intragallery; therefore there is almost no expansion of the interplanar spacing of the nanolayers for the e-beam-cured nanocomposite during the e-beam cure. So the morphology will retain the same gallery expansion as that before the-beam curing.

3.3 DYNAMIC MECHANICAL ANALYSIS

The dynamic mechanical analysis was performed on the e-beam-cured pure Epon 862/CD1012 and e-beam-cured 1.5 wt.% SiO_2/Epon 862 nanocomposite. The dynamic modulus and tan δ curves versus temperature of these two e-beam-cured materials are shown in Figure 6. The storage modulus of cured 1.5 wt.% SiO_2/Epon 862 nanocomposite has increased by ~10% in

the glassy state compared with that of the cured pure Epon 862/CD1012. Although the degree of cure for 1.5 wt.% SiO_2/Epon 862 nanocomposite is lower than the pure Epon 862/CD1012 (79% vs. 86%), the storage of the modulus of the nanocomposite is still higher, which should be the enhancement from the spherical silica nanoparticle. The tan δ curves show that the glass transition temperatures are 157°C and 154°C for the e-beam-cured pure Epon 862/CD1012 and e-beam-cured 1.5 wt.% SiO_2/Epon 862/CD1012 nanocomposite, respectively. Although the cure degree is not complete, the glass transition temperature is still very high. It is interesting to compare the modulus and glass transition temperature of the e-beam-cured epoxy with that of the thermally-cured system of Epon 862 with aromatic amine (curing agent W, diethyltolueneamine), which is a typical high-temperature aerospace epoxy. The dynamic modulus and tan δ curves versus temperature of the e-beam-cured Epon 828/CD1012 and the thermally-cured Epon 862/W are shown in Figure 7. Although the e-beam-cured Epon 828/CD1012 is not fully cured, the storage modulus of the e-beam-cured Epon 862/CD1012 was significantly higher than that of the thermally-cured Epon 862/W, and the glass transition temperature is very close. So, the e-beam technology is very promising in the application to the aerospace epoxy industry.

Similarly, the dynamic modulus and tan δ curves versus temperature of the e-beam-cured pure Epon 828/CD1012 and e-beam-cured 1.3 wt.% SiO_2/Epon 828 nanocomposite are shown in Figure 8. The storage modulus of cured 1.3 wt.% SiO_2/Epon 828/CD1012 nanocomposite has slightly increased in the glass state compared with that of cured pure Epon 862/CD1012. The tan δ curves show that the glass transition temperatures are 175°C and 176°C for the e-beam-cured pure Epon 828/CD1012 and e-beam-cured 1.5 wt.% SiO_2/Epon 862/CD1012 nanocomposite, respectively. Again in spite of incomplete cure, the glass transition temperature is very high and

~20°C higher than that of the thermally-cured aerospace epoxy resin (Epon 862/W). The relatively higher glass transition temperature for the Epon 828/CD1012 system than that of the Epon 862/CD1012 system is likely due to the relatively less flexible Epon 828 backbone than that of Epon 862.

4. CONCLUSIONS

This research demonstrates that layered-silicate epoxy nanocomposite and spherical silica epoxy nanocomposite can be successfully cured with an e-beam. This is an inspiring fusion of the fields of nanocomposite and e-beam curing technology. Based on DSC studies, the degree of cure is around 80% for the pure Epon 862 or Epon 828, 70 to 80% for the spherical silica epoxy nanocomposite and 60 to 70% for the layered-silicate epoxy nanocomposite. The characterization from TEM shows that the homogeneous dispersion of aggregated silica nanoparticle (~100 nm) in the spherical silica epoxy nanocomposite and intercalated or a combination of exfoliated and intercalated morphology in the e-beam-cured layered-silicate epoxy nanocomposite. The dynamic mechanical analysis studies show that the storage modulus of the e-beam-cured epoxy is higher than that of the thermally-cured Epon 862/W, and the glass transition temperature is higher or similar to that of Epon 862/W. Also, the addition of the silica nanoparticle can further increase the storage modulus in the e-beam-cured epoxy.

5. ACKNOWLEDGEMENT

This work is supported by the Air Force Research Laboratory, Materials & Manufacturing Directorate (Contract # FA8650-05-D-5052), and the Air Force Office of Scientific Research.

6. REFERENCES

1. Ellsworth, M. W.; Novak, B.M. *J. Am. Chem. Soc.* **1991,** *113,* 2756-2758.
2. Lee, A.; Litchenhan, J.D. *Macromolecules* **1998,** *31,* 4970-4974.
3. Alexandre, M.; Dubois, P. *Mater. Sci. and Eng.: R. Rep.* **2000**, *28,* 1-63.
4. Pinnavaia, T. J.; Beall, G. W. *Polymer-Clay Nanocomposites;* John Wiley & Sons, Ltd.: Chichester, UK, **2000.**
5. Tjong, S. C. *Mater. Sci. and Eng.: R. Rep.* **2006**, *53,* 73-197.
6. Hussain, F.; Hijjati, M.; Okamoto, M.; Gorga, R. E. *J. Compos. Mater.* **2006,** *40,* 1511-1575.
7. Wang, M.S.; Pinnavaia, T.J. *Chem. Mater.* **1994**, *6,* 468-474.
8. Lan, T.; Kavirayna, P.D.; Pinnavaia, T.J. *J. Phys. Chem. Solids* **1996***, 57,* 1005-1010.
9. Benson Tolle, T.; Anderson, D.P. *Com. Sci. and Tech.* **2002***; 62 (7-8),* 1033-1041.
10. Chen, J.S.; Poliks, M.D.; Ober, C.K.; Zhang, Y.; Wiesner, U.; Giannelis, E.P. *Polymer* **2002**, *43*, 4895-4904.
11. Chen, C.; Curliss, D. *Nanotechnology* **2003**, *14 (6),* 643-648.
12. Chen, C.; Curliss, D. "Preparation, characterization, and nanostructural evolution of epoxy nanocomposites" *J. Appl. Polym. Sci.* **2003,** *90 (8),* 2276-2287.
13. Becker, Ole; Cheng, Yi-Bing; Varley, Russell J.; Simon, George P. *Macromolecules* **2003**, *36 (5),* 1616-1622.
14. Chen, C.; Benson-Tolle, T. *J. Polym. Sci., Part B: Polym. Phys*. **2004,** *42 (21),* 3981-3986.
15. Wang, K.; Chen L.; Wu, J.; Toh, M.; He, C.; Yee, A. F. *Macromolecules* **2005,** *38,* 788-800.
16. Hutchinson, J.M.; Montserrat, S.; Roman, F.; Cortes, P.; Campos, L. *J. Appl. Polym. Sci.* **2006,** *102 (4),* 3751-3763.
17. Yasmin, A.; Luo, J.J.; Abot, J.L.; Daniel, I.M. *Composite Science Technology*, **2006,** *66 (14),* 2415-2422.
18. Kinloch, A.J.; Taylor, A.C. *J. Mater. Sci. Lett.,* **2003,** *22,* 1439-1441.
19. Liu, Y. L.; Hsu, C. Y.; Wei, W. L.; Jeng, R. J. *Polymer,* **2003,** *44 (18),* 5159-5167.

20. Sun, Y.; Zhang Z.; Moon, K.-S.; Wong C. P. *J. Polym. Sci.: Part B: Polym. Phys.* **2004,** *42,* 3849-3858.
21. Sun ,Y. Y.; Zhang, Z. Q.; Wong, C. P. *Polymer* **2005,** *46 (7),* 2297-2305.
22. Zhang, H; Zhang, Z.; Friedrich K.; Eger, C. *Acta Mater.,* **2006,** *54,* 1833-1842.
23. Seidel, J. R. *"Radiation Curing of Polymers,"* Randell, D. R., ed., The Royal Society of Chemistry, London, **1987.**
24. Beziers, D.; Perilleux, P.; Grenie Y. *Radiat. Phys. Chem.,* **1996,** *48,* 171-177.
25. Everett, J. P. ; Schmidt, D. L.; Rose, G.D.; Argritis, P.; Aidinis, C. J.; Hatzakis M. *Polymer* **1997,** *38 (7),* 1719-1726.
26. Lopata, V.; Sunders, C.; Singh, A.; Janke, C.; Wrenn, G.; Havens, S. *Radiat. Phys. Chem.* **1999,** *56,* 405-415.
27. Korenev, S. *Vacuum* **2001,** *62,* 233-236
28. Crivello, J. V. *Radiat. Phys. Chem.* **2002,** *63 (1),* 21-27.
29. Berejka, A. J.; Eberle, C. *Radiat. Phys. Chem.* **2002,** *63,* 551-556.
30. Crivello, J. V.; Ma, J. Q.; Jiang, F. M. *J. Polym. Sci. Part A Polym. Chem.* **2002,** *40 (20),* 3465-3480.
31. Mascioni, M.; Sands, J. M.; Palmese, G. R. *Nucl. Instrum. Methods Phys. Res. Sect. B* **2003,** *208,* 353-357.
32. Alessi, S.; Calderaro, E.; Parlato, A.; Fuochi, P.; Lavalle, A.; Corda, U.; Dispenza, C.; Spadaro. G. *Nucl. Instrum. Methods Phys. Res. Sect. B* **2005,** *236,* 55-60.
33. Bulut, U.; Crivello, J. V. *Macromolecules* **2005,** *38 (9),* 3584-3595.
34. Chen, C.; Curliss, D. *Polym. Bull.* **2003,** *49,* 473-480.
35. Chen, C., et al. Unpublished results.

Table 1. The curing degree of the e-beam-cured samples

Materials	Degree of Cure (%)
Epon 862/CD1012	86
Epon 828/CD1012	77
1.5 wt.% SiO_2/862/CD1012	79
1.3 wt.% SiO_2/828/CD1012	73
3.7 wt.% I.30E/862/CD1012	69
4.0 wt.% SC8/862/CD1012	67
1.0 wt.% S30B/862/CD1012	63

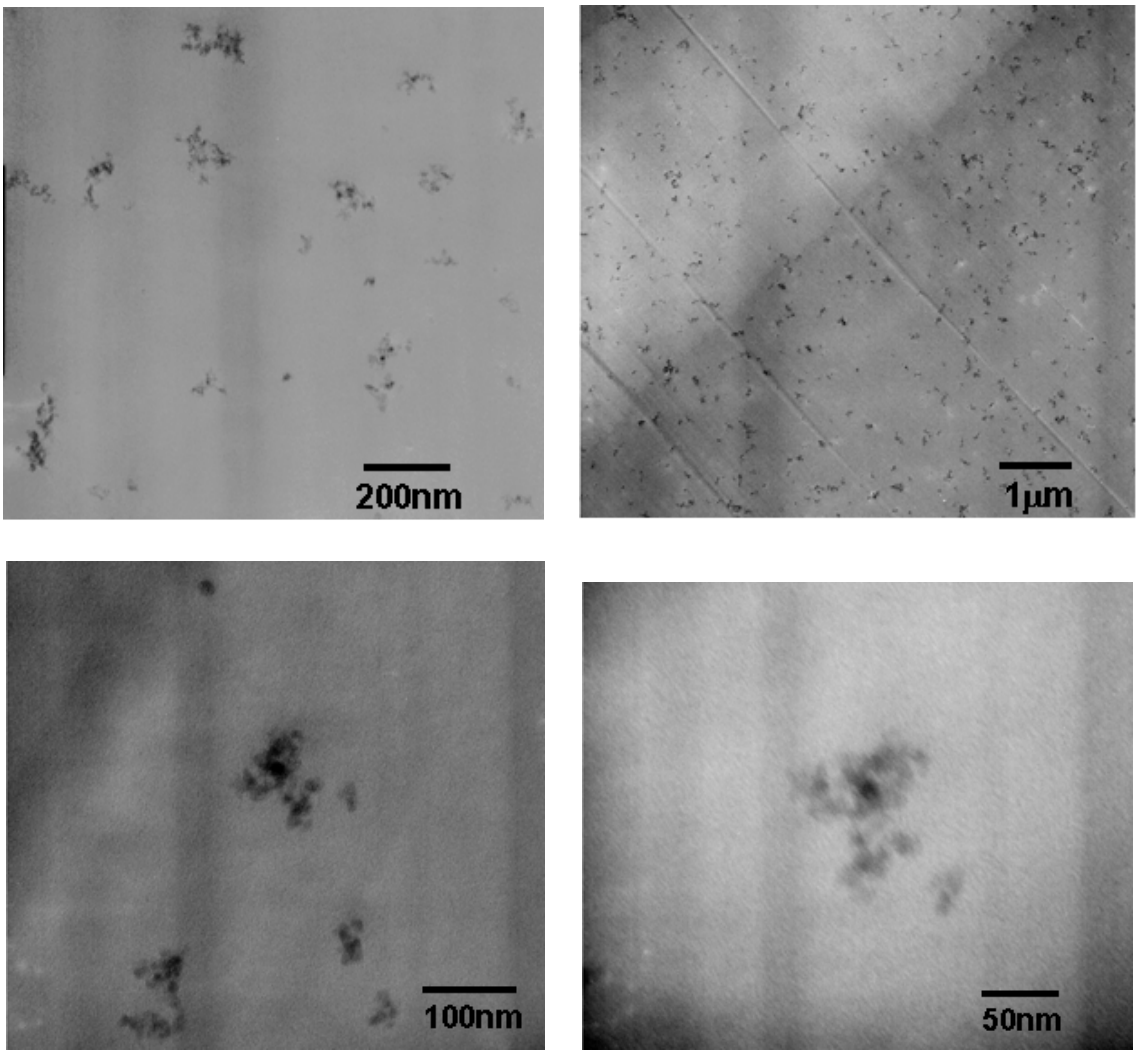

Figure 1. TEM images of the e-beam-cured 1.5 wt.% SiO_2/Epon 862/CD1012 nanocomposite.

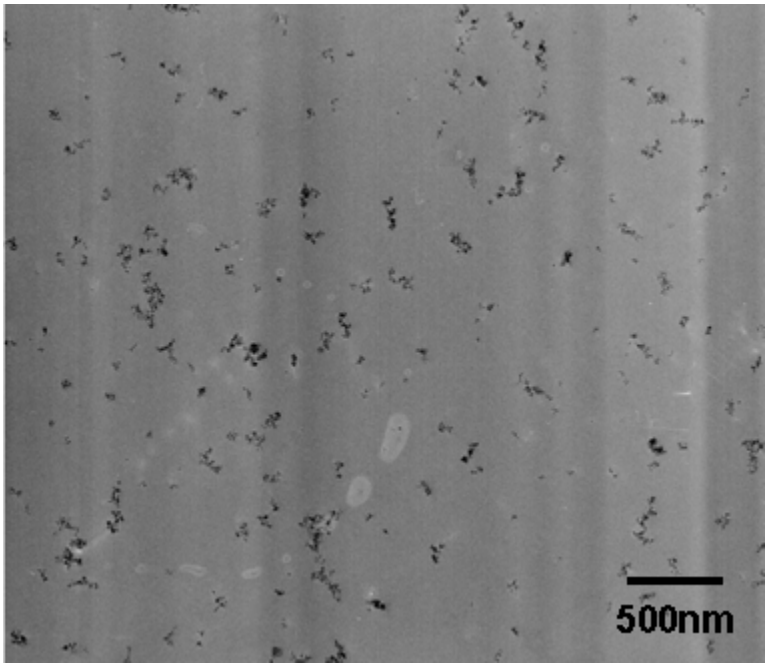

Figure 2. TEM image of the e-beam-cured 1.3 wt.% SiO_2/Epon 828/CD1012 nanocomposite.

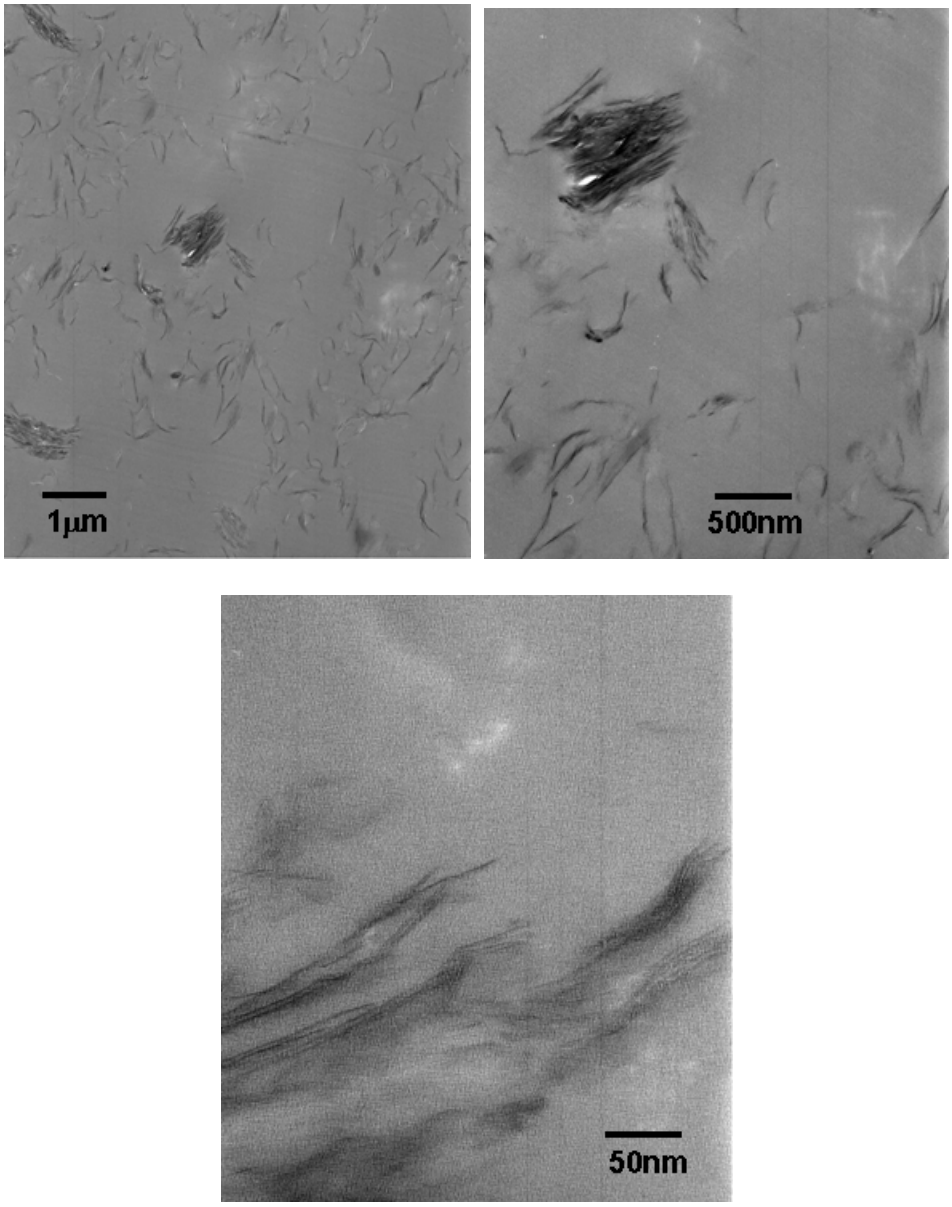

Figure 3. TEM images of the e-beam-cured 4 wt.% SC8/Epon 862/CD1012 nanocomposite.

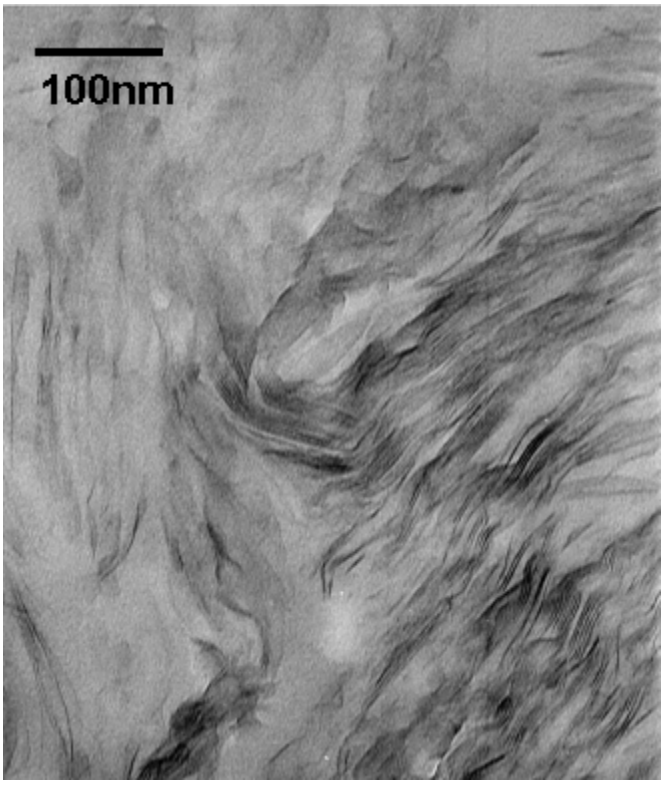

Figure 4. TEM image of the e-beam-cured 3.7 wt.% I.30E/Epon 862/CD1012 nanocomposite.

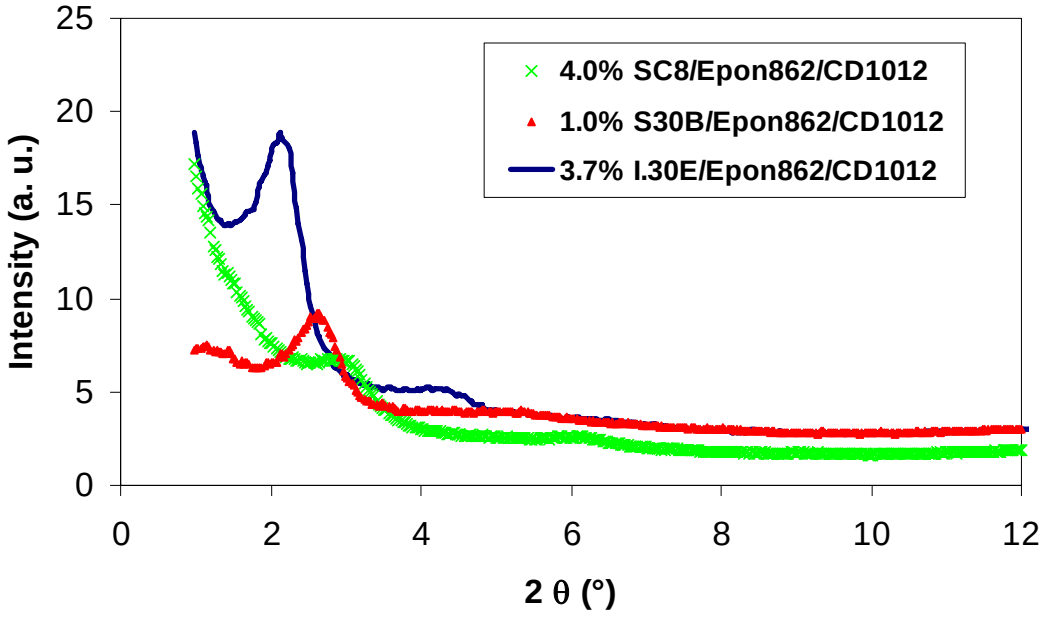

Figure 5. Small-angle x-ray scatterings of the e-beam-cured 4.0 wt.% SC8/Epon 862/CD1012 nanocomposite, 1.0 wt.% S30B/Epon 862/CD1012 nanocomposite, and 3.7 wt.% I.30E/Epon 862/CD1012 nanocomposite.

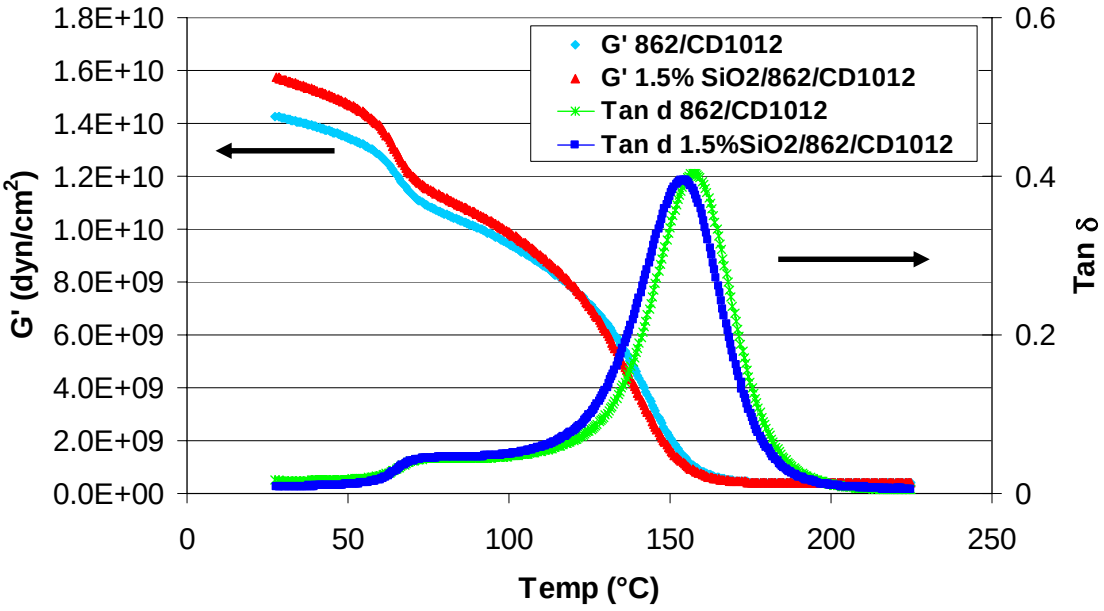

Figure 6. Dynamic storage modulus and tan δ curves (versus temperature) of the e-beam-cured pure Epon 862/CD1012 and 1.5 wt.% SiO_2/Epon 862/CD1012 nanocomposite.

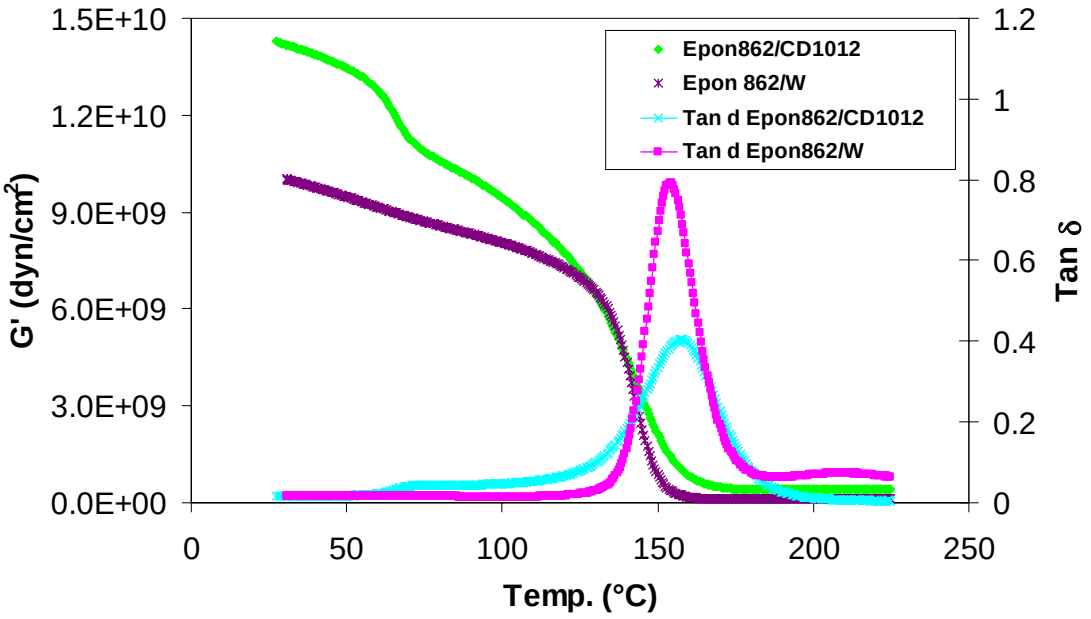

Figure 7. Dynamic storage modulus and tan δ curves (versus temperature) of the e-beam-cured pure Epon 862/CD1012 and thermally-cured Epon 862/W.

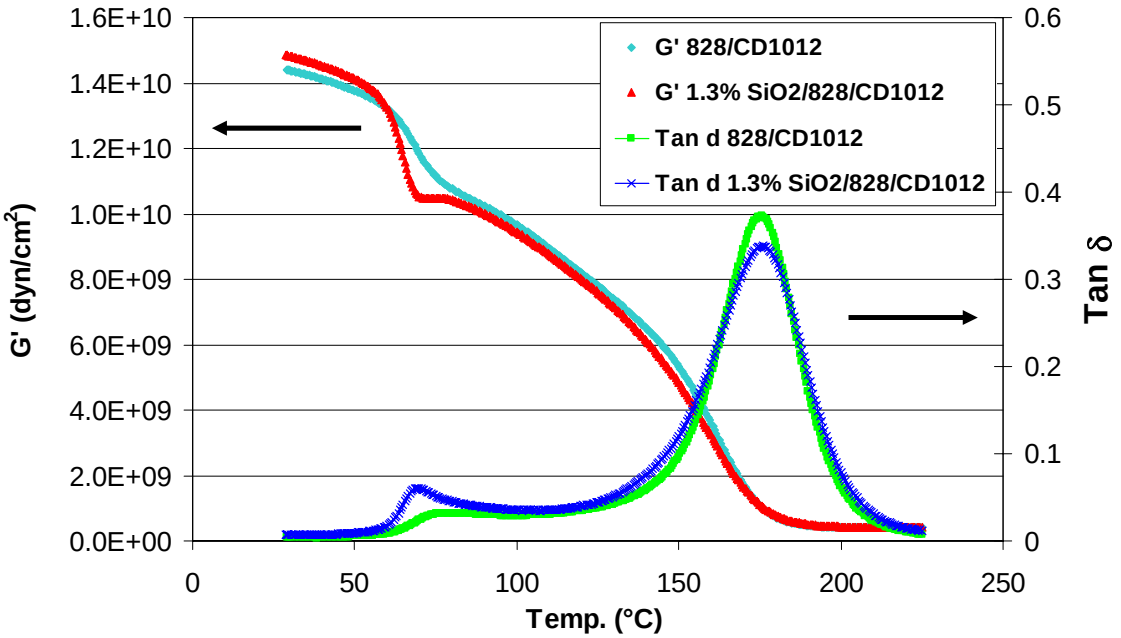

Figure 8. Dynamic storage modulus and tan d curves (versus temperature) of the e-beam-cured pure Epon 828/CD1012 and 1.3 wt.% SiO_2/Epon 828/CD1012 nanocomposite.